Egypt. J. Chem. **Vol.**, No. 10 pp. 5725 - 5734 (2021)

Egyptian Journal of Chemistry

http://ejchem.journals.ekb.eg/

One-Step Hydrothermal Synthesis of α- MoO_3 Nano-belts with Ultrasonic Assist for incorporating TiO_2 as a NanoComposite

Amani Jabbar Obaid and Luma Majeed Ahmed*

Department of Chemistry, College of Science, University of Kerbala, Kerbala- 56001, Iraq.

Abstract

One of the goals of this project was to utilize the hydrothermal method in preparation of α- MoO_3 nano-belts as bluish power at 180°C for 5h. This nanomaterial was incorporated with rutile-TiO_2 to produce a nanocomposite photocatalyst by a direct ultrasonic method in a ratio of 0.25(α-MoO_3): 9.75(TiO_2) as w/w ratio. The characterized of samples found by X-ray diffraction(XRD), scan electron microscopy(SEM), and ultraviolet-visible spectrophotometry. The XRD analysis and SEM image for prepared α-MoO_3 are proved the α-MoO_3 is prepared as a nano-belts, but its composite is being as spherical with elevated if roughness of its surface after incorporation. The bandgap of α-MoO_3 nanobelts increased from 2.8 eV to 2.95 eV after fabrication it surfaces with rutile-TiO_2 that attitude to the small Mo^{6+} ion incorporated with Ti^{4+} of TiO_2 matrix and both ions have a coordination number equal to 6 that enhanced this incorporation. XRD data indicated to all samples are having a nanosize, but SEM analysis proved all samples are polycrystals. The photocatalytic efficiency and the quantum yield for Chlorazol black BH dye decolorization using α-MoO_3 nano-belts were investigated under UV-A light and observed it elevated with using its nanocomposite. That is due to elevating the acidity of α-MoO_3 nano-belts surface after incorporating it in a rutile-TiO_2 crystal lattice, which decreases the recombination and increases the generalization of hydroxyl radical. The photoreaction for using α-MoO_3 nano-belts and its composite obeyed pseudo-first-order kinetics.

Keywords: Nano-belts; nanocomposite; hydrothermal method; α-MoO_3; TiO_2 and direct Blue 2.

1. Introduction

Growing applications have expanded the use of photocatalysts in alcoholic or aqueous solutions in various areas of human life. The photocatalyst work relies on the creation of reactive oxygen species (ROSs) (such as superoxide anion, hydrogen peroxide, and the hydroxyl radical) under artificial or solar light illumination [1-3]. Molybdenum trioxide (MoO_3) is known as a semiconductor of n-type, bluish-gray, or light yellow color, low cost, and has a direct bandgap(2.39-2.90) eV, which leads to being acted as a photocatalyst[4,5].In general, MoO_3 is contained on three crystalline structures with high stability relative to other metal oxide compounds, such as the thermodynamically stable orthorhombic phase (α-MoO_3), the metastable monoclinic phase (β-MoO_3), and the hexagonal phase (h-MoO_3). At 400 °C, the β-MoO_3 can be converted to α-MoO_3 [6].MoO_3 has gained a great deal of attention due to its various applications, such as gas sensing [7], catalyst [8], used in the manufacture of some organic photovoltaic cells[9], in the decolonization of dye[10,11], and used to improve the performance of lithium batteries [12]. Some researchers modified the surface of MoO_3 by fabricating it with other semiconductors like TiO_2 by physical mixing method then calcinated[13], via hydrothermal synthesis[14], via Microwave Method[15], and using sol-gel method[16]. This work proposes the synthesis of α-MoO_3 nano- belt using a hydrothermal method, and then incorporation with rutile- TiO_2 as a nanocomposite. The structure, morphology, and optical properties of the α-MoO_3-TiO_2 nanocomposite, and its use as a photocatalyst have also been investigated.

2. Experimental

Materials:

Rutile-TiO_2 was supplied by Riedel-De-Haen AG, Seelze, Hannover, Germany. Sodium molybdate dihydrate($Na_2MoO_4.2H_2O$), and Chlorazol black BH dye were purchased from Merck, Germany. Some

*Corresponding author e-mail: luma.ahmed@uokerbala.edu.iq
Receive Date: 18 April 2021, Revise Date: 25 May 2021, Accept Date: 26 May 2021
DOI: 10.21608/EJCHEM.2021.72582.3615

important properties of Chlorazol black BH dye ($C_{32}H_{21}N_6Na_3O_{11}S_3$) with Molecular weight 830.71 g mol^{-1} were shown in **Table1**. The rest chemical materials were used without any further purification processes.

Table 1. Some properties of Chlorazol black BH dye[17].

IUPAC name	Trisodium,5-amino-3-[[4-[4-[(7-amino-1-hydroxy-3sulfonatonaphthalen-2-yl)diazenyl]phenyl]phenyl]diazenyl]-4-hydroxynaphthalene-2,7 disulfonate.
Synonym	Direct Blue 2
Structure formula	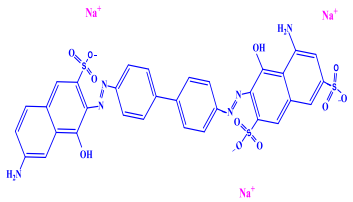
Class	Azo dyes
λ_{max}	500-550 nm

A. Instruments

The batch home-made reactor was used to perform the photoreaction experiments. The illumination was carried out high-pressure mercury lamp (HPML- Radium 400 W) at λ_{max} = 365 nm.

Procedure

Synthesis of MoO_3 nanobelt

α-MoO_3 nanobelt was prepared using sodium molybdate dihydrate as a precursor with dilution HCl. This mixture was transferred to steeliness steel Teflon tube autoclave and put in the oven at 180 ºC for 5 h. After cooling at room temperature, the product was filtered and washed with distilled water and absolute ethanol three times to ensure removing the non-reactive materials. The bluish-gray product was dried in an oven at 80 ºC for 1 h and then stored overnight in a desiccator. The step of α-MoO_3 synthesis using the hydrothermal method is shown in **figure.1**.

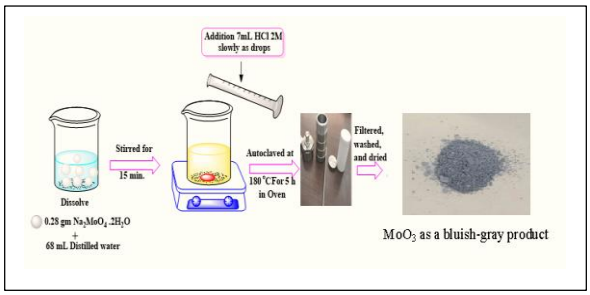

Fig. 1. The schematic diagram for the steps of α-MoO_3 synthesis using the hydrothermal method.

The chemical equations of α-MoO_3 Synthesis were followed below.

$$Na_2MoO_4.2H_2O + 2HCl \rightarrow H_2MoO_4 + 2NaCl + 2H_2O \ldots(1)$$

$$H_2MoO_4 \rightarrow MoO_3 + H_2O \quad \ldots(2)$$

Synthesis of α-MoO_3/TiO_2 nanocomposite

The 0.25(α-MoO_3): 9.75(TiO_2) nanocomposite was prepared as w/w ratio using ultrasonic wave. The α-MoO_3 solution and TiO_2 solution were dispersed for 3h at 70 ºC using ultrasonic waves at 60 kHz. The α-MoO_3 solution was gradually added to TiO_2 solution and going on for 1h at 70 ºC to perform the binding process between Mo and Ti. The produced suspension was mixed on a magnetic stirrer at 70 ºC until evaporating all ethanol. The precipitate was washed and filter with water and ethanol, then stored overnight in a desiccator. The steps of the composite are explained in **figure 2.** According to equation 3, the suggested chemical equation for the Synthesis of α-MoO_3/TiO_2 nanoparticles was obtained.

$$MoO_3 + TiO_2 \xrightarrow{ultrasonic\ waves} MoO_3 - TiO_2 \quad \ldots(3)$$

Fig. 2. The schematic diagram for the steps of α-MoO_3/TiO_2 composite using ultrasonic waves.

photoreaction of* Chlorazol black BH *dye with synthesis photocatalysts

The application of these catalysts was performed using in decolorization of Chlorazol black BH dye.

This photoreaction was applied using a homemade photoreactor in **figure 3**. This photoreactor consists of 400 watts Philips UV-A lamp with an intensity of light equal to 2.95 x10^{-7} Einstein.s^{-1}, the body of the reactor manufactures from a wooden box, which contains an inside magnetic stirrer, Pyrex glass beaker (500 mL), Teflon bar, and fan.

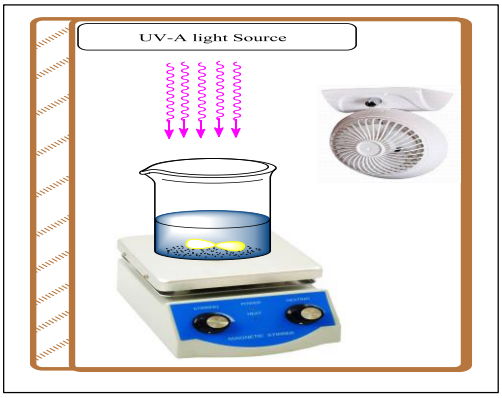

Fig. 3. Schematic diagram of Homemade Photocatalytic Reactor Unit.

A 100 mg of studied photocatalysts was mixed with 50 ppm of Chlorazol black BH dye at 18 ºC and initial pH of dye 7.6. Without irradiation, the produced suspension solution was magnetically stirred for 30 min to allow for an equilibrium adsorption state to be reached. After the adsorption step, the UV-light was applied onto this suspension, and then about 3 mL aliquots were collected at intervals of time of irradiation until 100 min. The collected suspensions were separated twice times by centrifuge for 20 min, the absorption of the produced filters was recorded at 500 nm using Uv-Visible spectroscopy. The rate constant ($k_{app.}$)and photo-decolorization efficiency percentage (PDE%) were determined depending on the initial concentration of dye (C_o) at the adsorption process and residue dye concentration (C_t) under irradiation by the following equations[18-27].

$$\ln\left(\frac{C_o}{C_t}\right) = k_{app}t \qquad \ldots (4)$$

$$PDE\ \% = \frac{(C_o - C_t)}{C_o} \times 100 \qquad \ldots (5)$$

3.Results and Discussion

A.Structural Properties

Based on **figure 4**. For all photocatalyst samples, XRD analysis was performed to investigate the structure of samples using 2θ ranging from 20º to 80º using Lab X XRD 6000-Shimadzu.

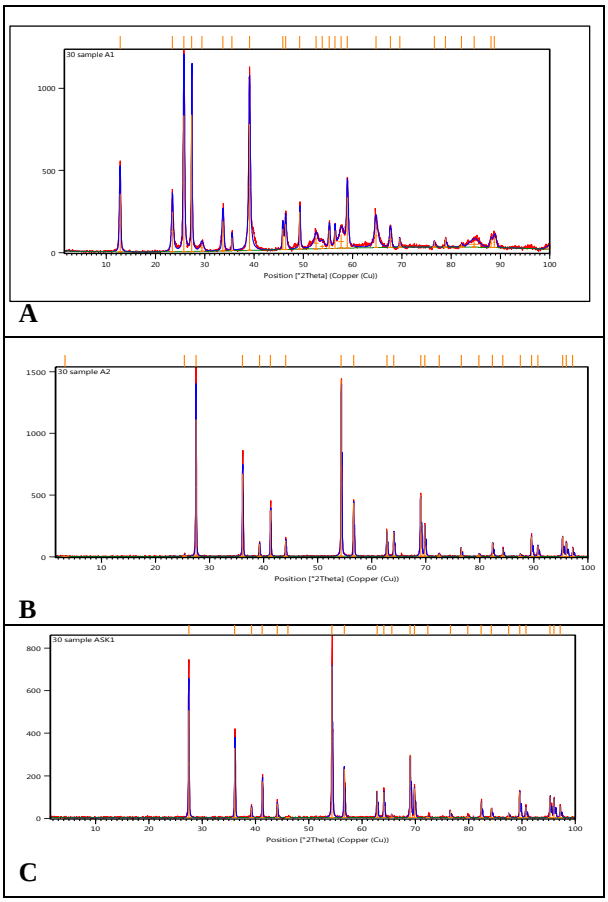

Fig. 4. XRD patterns of α-MoO_3(a), TiO_2 (b), and α-MoO_3/TiO_2 nanocomposite (c).

The synthesis α-MoO_3 is identified as orthorhombic(α- MoO_3) in figure 4, and agrees with the standard diffraction data of α- MoO_3 (JCPDS Card No. 005-0508)[28]. The essential diffraction peaks of orthorhombic MoO_3 appear at 12.80◦, 25.76◦, 27.35◦, 39.059◦, 58.906◦ and 67.630◦ with miller indicates (0 2 0), (0 4 0), (021),(0 6 0), (0 8 1) and (0 10 0) planes respectively, and they strongly agreement with results in references[28,29]. Moreover, the stronger intensity at 2θ for 12.8º, 25.7º, and 39.0º of the reflection peaks of (0 k 0) with k 2, 4, 6 indicates the anisotropic growth of the nanobelts[29]. However, the rutile-TiO_2 peaks appear at diffractions (110), (101), (111), (211), (220) and (301) with 2θ positions are 27.46°, 36.10°, 41.26°, 54.34°, 56.32°, and 69.02° respectively, these results are agreement with the standard diffraction data (JCDS card No.00-021-1276)[30,31]. When the α- $MoO_3$and rutile TiO_2 incorporate as nanocomposite, some essential peaks are shifted toward the high 2θ from 27.358º (α-MoO_3) and 27.475º (TiO_2) to 27.480º, from 36.118º (TiO_2) to 36.122º, from 39.059º (α-MoO_3) to 39.230º, 41.279º (TiO_2) to 41.287º. That attitude generates a metallic bond between two metals [32-

34]. The Mo^{6+} is suitable to incorporate with Ti^{4+} in crystal lattice because both have a coordination number of 6 [13], Mo ion is small compared with Ti and has an ionic radii 0. 59 Å[35] and 0.67 Å[36] respectively.

On the other side, the mean crystal sizes (L) for all samples were calculated by utilizing Scherer's equations [37-40]. Where k, λ,β and θ are indicated to shape constant, the wavelength of Cu, Bragg diffraction angle, and full width at half maximum intensity (FWHM).

$$L = \frac{k\,\lambda}{\beta\ Cos\ \theta} \qquad \ldots\ (6)$$

The results indicate to all samples are having a nano-size, and the mean crystal size of α-MoO_3 elevates with incorporating the TiO_2 from 30.5511 nm to 57.6063 nm, because the rutile-TiO_2 has a maximum value of mean crystal size and equal to 72.3799 nm.

B.Morphology of studied photocatalyst surfaces

The morphology of the sample's surface was estimated using SEM analysis (FESEM FEI Nova Nano SEM 450). **Figure 5** explains the SEM images for α-MoO_3, TiO_2, and its nano-composite surfaces and found that the shape of synthesis α-MoO_3 is nano-belts, this result is in agreement with the result of XRD and works of literature [28,29]. The rutileTiO_2 and composite appear spherical because the amount of TiO_2 is very high compared with the amount of α-MoO_3 to increase the lightness of α-MoO_3. The partial sizes of α-MoO_3 and its composite are not in nano-size that refers to the poly-crystal. TiO_2 is a commercial material with a micro-size

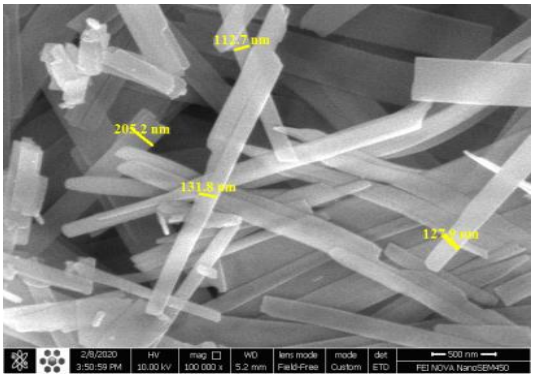

A

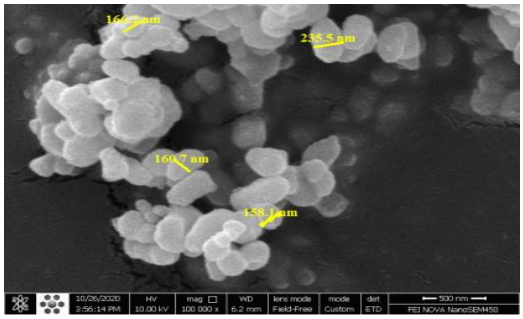

B

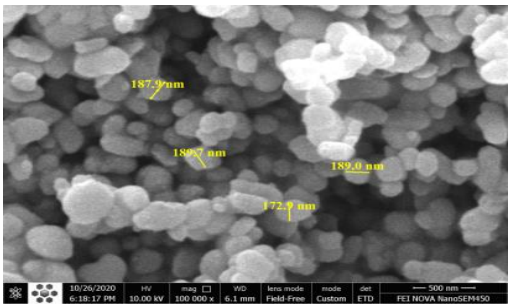

C

Fig. 5. SEM images of α-MoO_3(a), TiO_2(b), and α-MoO_3/TiO_2 composite(c).

C. Optical property of studied photocatalyst

The optical energy bandgap (Eg in eV) for all photocatalyst samples was measured with basing on Tauc equation[30,37]. Where α , h, v, k, t, A, and m are absorption coefficient, Plank's constant the light, frequency, optical constant, thickness, the absorbance and constant value equal to ½ or 2 for direct and indirect transitions, respectively.

$$\alpha hv = k(hv - Eg)^m \qquad \ldots\ (7)$$

$$\alpha = (2.3026\ A)/t \qquad \ldots\ (8)$$

According to the plotted Tauc equation in **Figures 6**, **7, and 8**, that observed the bandgap for α-MoO_3 is direct, but it is an indirect bandgap for the TiO_2 and α-MoO_3/TiO_2 nanocomposite with magnitudes equal to 2.8 eV, 3 e V and 2.95 e V respectively.

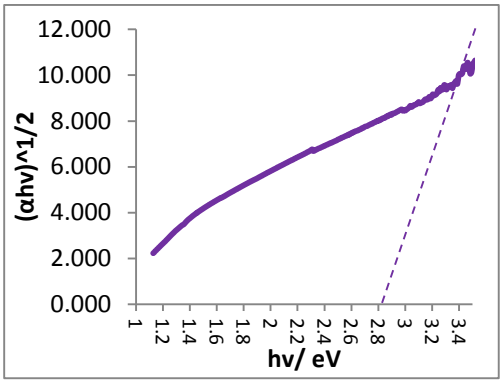

A

Fig. 6. Tauc plot for α-MoO_3 as a direct bandgap.

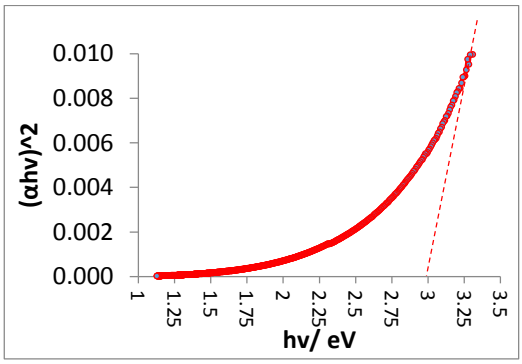

B

Fig. 7. Tauc plot for TiO_2 as an indirect bandgap.

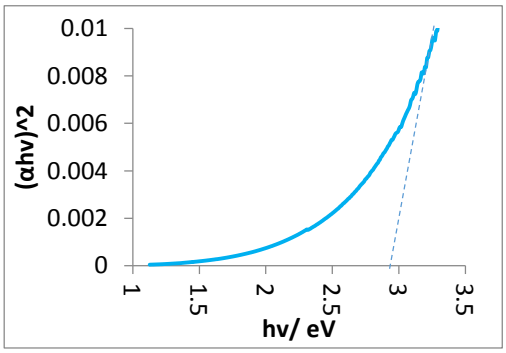

C

Fig. 8. Tauc plot for (α-MoO_3/ TiO_2) nanocomposi-tes as an indirect band gap.

D. Photo-decolorization of Chlorazol black BH dye

After ensure from the prepared α-MoO_3 nanobelt and its nanocomposite with rutile-TiO_2 were applied in Chlorazol black BH dye solution to study the efficiency of. **Figures 9 and 10** indicate the apparent rate constant and PDE% for Chlorazol black BH dye decolorization using α-MoO_3 nanobelts elevate with incorporating it with TiO_2. The PDE% of α-MoO_3 nanobelt increase from 46.29 % to 56 .54% for its composite at 100 min irradiation for 50 ppm of dye with 100 mg of sample. That attitude increases the lightness of α-MoO_3 nanobelts and elevates the acidity of its surface via the synthesis of its composite that leads to an increase in the adsorption of hydroxyl ions[30,33], which generate hydroxyl radicals under irradiation by UV light or visible light[41-43]. Moreover, this modification of the surface will increase the separation of changes on photocatalyst and increase the electron-hole recombination time [37].

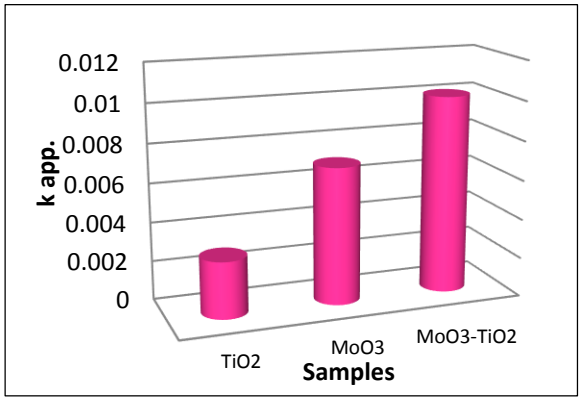

Fig. 9. The relation between the apparent rate constant for Chlorazol black BH dye decolorization in studied photocatalyst solution.

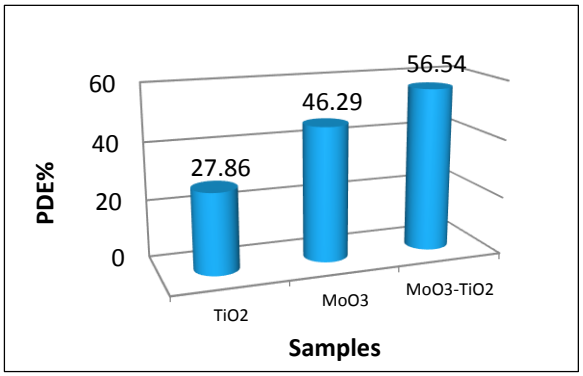

Fig. 10. The relation between PDE% for Chlorazol black BH dye decolorization in studied photocatalyst solution

E. Quantum yield of photo decolorization of Chlorazol black BH dye

The quantum yield is expressed on the efficiency of photocatalytic reaction, which depended on the number of probe dye molecules that degrade per photon absorbed [44,45]. Under using UV-A lamp, the quantum yield (Φ) can be determined using the $k_{app.}$ (in sec^{-1}) of the pseudo-first-order of Chlorazol black BH dye photodecolorization with light intensity (Io) via the following equation[46-48].

$$\Phi = \frac{k_{app.}}{2.303\ I_o\ \varepsilon\ l} \quad \ldots (9)$$

where: ε is the molar absorptivity of Chlorazol black BH dye (84.469 mol^{-1} L cm^{-1}) and l is cell path length term (cm).

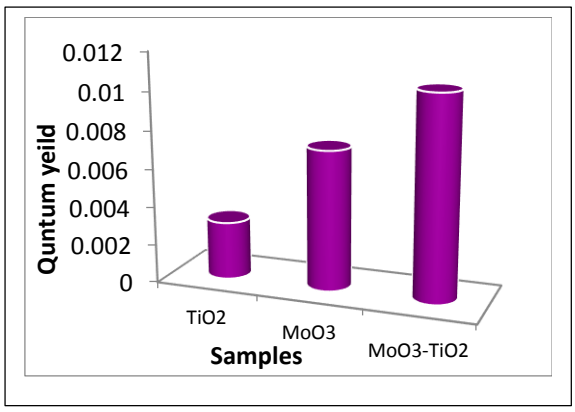

Fig. 11. The relation between the quantum yield of Chlorazol black BH dye photodecolorization with studied samples.

As seen in **figure. 11**, the quantum yield of Chlorazol black BH dye decolorization is elevated to the following sequence:

Φ using α- MoO_3/TiO_2 naanocomposite > Φ using α-MoO_3 nanobelts > Φ using rutile-TiO_2

and equal to 0.010, 0.007and 0.003 respectively. The minimum quantum yields value is observed during using TiO_2 and α-MoO_3 nanobelts, that due to recombination processes that caused reversible reactions, may be produced quencher materials, a dimerization of dye molecules, and photophysical deactivation processes (ISC process) [45-47].

E. Suggested Mechanism

The proposed mechanism for any photocatalytic reaction is essentially dependent on products of the active species such as superoxide anion, peroxide radical, and hydroxyl radical in solution or on the surface of photocatalyst[48-52]. These species are altered in potential power to decolorize and disintegrate any organic colored materials. Hydroxyl radical is a more active species in an aqueous solution with 2.8 V, hence it acts as a powerful oxidant to attack the dye molecules [53-60]. The suggested chlorazol black BH decolorization was displayed in **figure.12** that mention in reference [17].

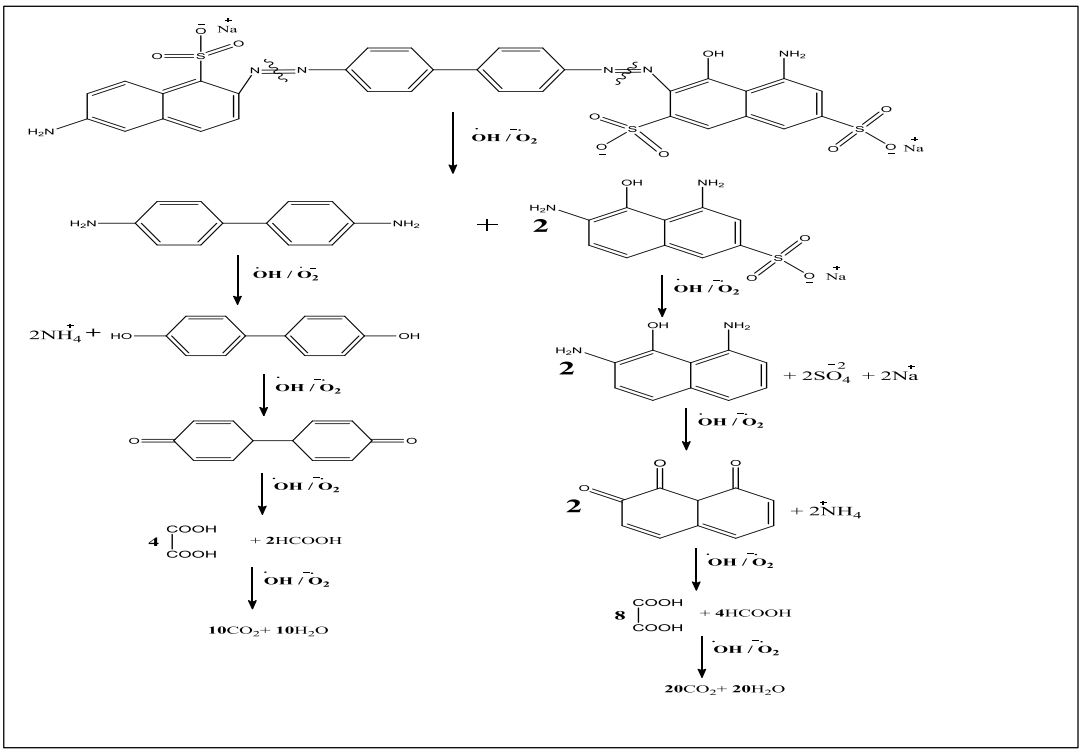

Fig. 12. Schematic diagram for decolorization and degradation of Chlorazol black BH dye in the photocatalytic system.

E. Conclusion

The α-MoO_3 was grown by the one-step hydrothermal method as nanobelts. The incorporation of α-MoO_3 with rutile-TiO_2 as nanocomposite was done using ultrasonic waves as an environment-friendly method. The prepared photocatalysts were conformed with XRD analysis, SEM, and optical bandgap. The XRD patterns indicate the formation of α-MoO_3 as an orthorhombic phase with nano size. SEM image obtained the synthesized α-MoO_3 is nanobelts and agreement with the miller indicates in XRD analysis. The optical band gap of α-MoO_3 elevated with incorporating in rutile- TiO_2 crystal lattice. The acidity of α-MoO_3 surface elevates via incorporating with rutile- TiO_2 crystal lattice and caused the increase in the photoreaction activity and quantum yield of Chlorazol black BH dye decolorization.

E. Conflicts of interest

"There are no conflicts to declare".

F. Formatting of funding sources

Self

G. Acknowledgments:

The authors are very much grateful to the college of the science of Kerbala University to enhance this MSC project in our MSC's Lab.

3.References

[1] Ahmed, L. M., Bulk and Nanocatalysts Applications in Advanced Oxidation Processes, Oxidoreductase, IntechOpen, DOI: http://dx.doi.org/10.5772/ intechopen.94234, 1-15, (2020).

[2] Collin, F., Chemical Basis of Reactive Oxygen Species Reactivity and Involvement in Neurodegenerative Diseases. *Int. J. Mol. Sci*., **20**(2407), 1-1, (2019), **https://doi.org/10.3390/ijms20102407**.

[3] Ahmed, L. M. and Hussein, F., Roles of Photocatalytic Reactions of Platinized TiO_2 Nanoparticales. 1st ed. LAP Lambert Academia Published; 2014. 103 P. ISBN-10: 3659538817.

[4] Bhatia, S. and Khanna, A., Structural and Optical Properties of Molybdenum Trioxide Thin Films, *Solid State Physics, AIP Conf. Proc.*, **1665**, 080057-1-080057-3(2015), https://doi.org/10.1063/1.4917961.

[5] Kanneganti, A., Manasa, C., and Doddapaneni, P., A Sustainable Approach Towards Synthesis of MoO_3 Nanoparticles using Citrus Limetta Pith Extract, *International Journal of Engineering and Advanced Technology (IJEAT*), **3**(5), 249 – 8958(2014).

[6] Chen, X., Lei, W., Liu, D., Hao, J., Cui, Q. and Zou, G., Synthesis and Characterization of Hexagonal and Truncated Hexagonal Shaped MoO_3 Nanoplates, *J. Phys. Chem. C*., **113**, 21582–21585 (2009), https://doi.org/10.1021/jp908155m.

[7] Nagyné-Kovács, T., Studnicka, L., Lukács, I. E., László, K., Pasierb, P., Szilágyi, I. M., and Pokol, G., Hydrothermal Synthesis and Gas Sensing of Monoclinic MoO_3 Nanosheets, *Nanomaterials*, **10**, 891, 1-12 (2020), https://doi.org/10.3390/nano10050891.

[8] Malakooti, R., Shafie, S., Hosseinabadi, R., Heravi, M. M., Zakeri, M., & Mohammad, N., MoO_3 Nanoparticles Synthesis via Hydro-Solvothermal Technique and Its Application as Catalyst for Efficient Ring Opening of Epoxides With Amines Under SolventFree Conditions, *Synthesis and Reactivity in Inorganic, Metal-Organic, and Nano-Metal Chemistry*, **44**, 1401–1406 (2014), https://doi.org/10.1080/15533174.2013.809740.

[9] Tseng, Y.C, Mane, A.U., Elam, J.W, Darling, S.B., Ultrathin molybdenum oxide anode buffer layer for organic photovoltaic cells formed using atomic layer deposition. *Sol. Energy Mater. Sol. Cells*, **99**, 235–239 (2012), https://doi.org/10.1016/j.solmat.2011.12.004.

[10] Murthy, T. N., Suresh, P., and Rao, A.V. P., Enhancement of visible light photocatalytic activity of MoO_3 with V_2O_5 additive, *International Journal of Engineering and Applied Sciences (IJEAS)*, **2**(11), 8-10 (2015).

[11] Chithambararaj, A., Sanjini, N. S., Bose, A. C., and Velmathi, S., Flower-like hierarchical h-MoO_3: new findings of efficient visible-light-driven nano photocatalyst for methylene blue degradation, *Catal. Sci. Technol.*, 1-10 (2013).

[12] Mai, L., Hu, B., Chen, W., Qi, Y., Lao, C., Yang, R., Dai, Y., and Wang, Z. L., Lithiated MoO_3 Nanobelts with Greatly Improved Performance for Lithium Batteries, *Adv. Mater*., **19**, 3712–3716 (2007), https://doi.org/10.1002/adma.200700883.

[13] Silvestri, S., Kubaski, E. T., Sequinel, T., Pianaro,S. A., Varela, J. A., and Tebcherani, S. M., Optical Properties of the MoO_3-TiO_2 Particulate System and Its Use as a Ceramic Pigment, Particulate Science and Technology, *An International Journal*, **31**(5), 466-473 (2013), https://doi.org/10.1080/02726351.2013.773388.

[14] Wang, C.; Wu, L.; Wang, H.; Zuo, W.; Li, Y.; Liu, J. Fabrication and Shell Optimization of Synergistic TiO_2 -MoO_3 Core-Shell Nanowire Array Anode for High Energy and Power Density Lithium-Ion Batteries, *Adv. Funct. Mater.* **25**,

3524–3533 (2015), https://doi.org/10.1002/adfm.201500634.

[15] Kubiak, A., Wojciechowska, W., Kurc, B., Pigłowska, M., Synoradzki, K., Gabała, E., Moszy´nski, D., Szybowicz, M., Siwi´nska-Ciesielczyk, K., and Jesionowski, T., Highly Crystalline TiO_2-MoO_3 Composite Materials Synthesized via a Template-Assisted Microwave Method for Electrochemical Application, *Crystals*, **10**(493), 1-25 (2020), https://doi.org/10.3390/cryst10060493.

[16] Dighore, N., Dhonde, S., Gaikwad, S., and Rajbhoj, A., Synthesis of conducting polymer Polypyrrole-MoO_3 nanocomposites, Mor. J. Chem., **4** (3), 797-804 (2016), https://doi.org/10.48317/IMIST.PRSM/morjchem-v4i3.5390.

[17] Abbas, S. K., Hassan, Z. M., and Ahmed, L. M., Influencing the Artificial UV-A light on decolorization of Chlorazol black BH Dye via using bulk ZnO Suspensions, *IOP Conf. Series: Journal of Physics: Conf. Series*, **1294**, 1-8 (2019). doi:10.1088/1742-6596/1294/5/052050.

[18] Mashkour, M., Al-Kaim, A., Ahmed, L., and Hussein, F., Zinc Oxide Assisted Photocatalytic Decolorization of Reactive Red 2 Dye, *Int. J. Chem. Sci.*, **9**(3), 969-979 (2011).

[19] Kzar, K.O., Mohammed, Z.F., Saeed, S.I., Ahmed, L.M., Kareem, D.I., Hadyi, H., and Kadhim, A. J., Heterogeneous photo-decolourization of cobaltous phthalocyaninate dye (reactive green dye) catalyzed by ZnO, In *AIP Conference Proceedings*, AIP Publishing LLC, 2144(1)020004020004-01 -020004-10 (2019), https://doi.org/10.1063/1.5123061.

[20] Abass, S. K., Al-Hilfi, J. A., Abbas S. K., and Ahmed, L. M., Preparation, Characterization and Study the Photodecolorization of Mixed-Ligand Binuclear Co (II) Complex of Schiff Base by ZnO, *Indones. J. Chem.*, **20**(2), 404 – 412 (2020), DOI: 10.22146/ijc.44192.

[21] Marhoon, A. A., Saeed, S. I., and Ahmed, L. M., Application of some effects on the Degradation of the aqueous solution of Fuchsine dye by photolysis, *Journal of Global Pharma Technology*, **11**(9), 76-81 (2019).

[22] Ahmed, L. M., Photo-Decolourization Kinetics of Acid Red 87 Dye in ZnO Suspension Under Different Types of UV-A Light, *Asian J. Chem.*, **30**(9), 2134-2140 (2018), DOI: 10.21275/ART20163016.

[23] Zuafuani S. I. S., and Ahmed, L. M., photocatalytic Decolourization of Direct Orange Dye Zinc Oxide Under Irradiation, *Int. J. Chem. Sci.*, **13**(1), 187-196 (2015).

[24] Alattar, R. A., Hassan, Z. M., Abass, S. K., and Ahmad, L. M., Synthesis, Characterization and Study the Photodecolorization of Schiff Base Fe(III) Complex in ZnO/Uv-A Light System, AIP Conference Proceedings, **2290**, 0300321-03003210 (2020), https://doi.org/10.1063/5.0027611.

[25] Karam, F. F., Saeed, N. H., Al-Yasari, A. H., Ahmed, L. M., and Saleh, H., Kinetic Study for Reduced the Toxicity of Textile Dyes (Reactive yellow 14 dye and Reactive green dye) Using UV-A light/ZnO System, *Egypt. J. Chem.*, **63**(8), 1-12 (2020), DOI: 10.21608/ejchem.2020.25893.2511.

[26] Jaafar, M. T., and Ahmed, L. M., Reduced the Toxicity of Acid Black (Nigrosine) Dye by Removal and Photocatalytic Activity of TiO_2 and Studying the Effect of pH, Temperature, and the Oxidant Agents, AIP Conf. Proc., **2290**, 030034-1– 030034-11 (2020), https://doi.org/10.1063/5.0027512.

[27] Alattar, R.A., Saleh, H. M., AL-Hilfi, J.A., and Ahmed, L.M., Influence the addition of Fe^{2+} and H_2O_2 on removal and decolorization of textile dye (dispersive yellow 42 dye), *Egypt. J. Chem.*, **63** (9), 3191-3201(2020), DOI: 10.21608/ejchem.2020.23542.2400 .

[28] Rahmani, M.B., Keshmiri, S.H., Yua, J., Sadek, A.Z., Al-Mashat, L., Moafic, A., Latham, K., Li, Y.X., Wlodarski, W., and Kalantar-zadeh, K., Gas sensing properties of thermally evaporated lamellar MoO_3, *Sensors and Actuators B*, **145**, 13–19 (2010), https://doi.org/10.1016/j.snb.2009.11.007.

[29] Ding, Q.P., Huang, H.B., Duan, J.H., Gong, J.F., Yang, S.G., Zhao, X.N., and Du, Y.W., Molybdenum trioxide nanostructures prepared by thermal oxidization of molybdenum, *J. Cryst. Growth*, **294** (2), 304–308 (2006), https://doi.org/10.1016/j.jcrysgro.2006.07.004.

[30] Jawad, T.M., and Ahmed, L. M., Direct Ultrasonic Synthesis of WO_3/TiO_2 Nanocomposites and Applying them in the Photodecolorization ofEosin Yellow Dye, *Periódico Tchê Química*, **17**(34), 621-633 (2020),.

[31] Filippo, E., Carlucci, C., Capodilupo, A. L., Perulli, P., Conciauro, Corrente, F., G. A., Gigli, G., and Ciccarell, G., Enhanced Photocatalytic Activity of Pure Anatase TiO_2 and Pt-TiO_2 Nanoparticles Synthesized by Green Microwave Assisted Route, *Materials Research*., **18**(3), 473-481 (2015), https://doi.org/10.1590/1516-1439.301914.

[32] Mohammed, B. A., and Ahmed, L. M., Improvement the photo-catalytic properties of ZnS nanoparticle with loaded manganese and

chromium by co-precipitation method, *JGPT*, **10**(7), 129-138 (2018).

[33] Hayawi, M. K., Kareem, M. M., and Ahmed, L. M., Synthesis of Spinel Mn_3O_4 and Spinel Mn_3O_4/ZrO_2 Nanocomposites and Using Them in Photo-Catalytic Decolorization of Fe(II)-(4,5-Diazafluoren-9-One 11) Complex. *Periódico Tchê Química*, **17**(34), 689- 699 (2020).

[34] Mahammed, B. A., and Ahmed, L. M., Enhanced Photocatalytic Properties of Pure and Cr-Modified ZnS Powders Synthesized by Precipitation Method, *Journal of Geoscience and Environment Protection*, **5,** 101-111, (2017), https://doi.org/10.4236/gep.2017.510009 .

[35] Shannon, R., Revised effective ionic radii and systematic studies of interatomic distances in halides and chalcogenides, *Acta Crystallographica A*, **32**(5),751–767 (1976), https://doi.org/10.1107/S0567739476001551.

[36] Ahmed, L.M., Ivanova, I., Hussein, F.H., and Bahnemann, D.W., Role of platinum deposited on TiO_2 in photocatalytic methanol oxidation and dehydrogenation reactions, *International Journal of Photoenergy*, 1-10 (2014), https://doi.org/10.1155/2014/503516 .

[37] Fakhri, F. H., and Ahmed, L. M., Incorporation CdS with ZnS as nanocomposite and Using in Photo-Decolorization of Congo Red Dye, *Indones. J. Chem.* , **19**(4), 936–943 (2019), https://doi.org/10.22146/ijc.38335 .

[38] Ahmed, L. M., Hussen, F. H., and Mahdi, A. A., Photocatalytic Dehydrogenation of Aqueous Methanol Solution by Naked and Platinized TiO_2 Nanoparticles, *Asian Journal of Chemistry*, **24**(12), 5564-5568 (2012).

[39] Fadhil, E. S., and Ahmed, L.M., and Mohammed, A. F., Effect of silver doping on structural and photocatalytic circumstances of ZnO nanoparticles, *Iraqi Journal of Nanotechnology, synthesis and application*, **1**, 13-20 (2020**),** https://doi.org/10.47758/ijn.vi1.22.

[40] Jassim, S., Abbas, A., AL-Shakban, M., and Ahmed, L., Chemical Vapour Deposition of CdS Thin Films at Low Temperatures from Cadmium Ethyl Xanthate/ acceptance in Egyptian Journal of Chemistry, **64**(5), 1-4, (2021), DOI: 10.21608/EJCHEM.2021.60695.3451 **.**

[41] Hussain, Z. A., Fakhri, F. H., Alesary H. F., and Ahmed, L. M., ZnO Based Material as Photocatalyst for Treating the Textile Anthraquinone Derivative Dye (Dispersive Blue 26 Dye): Removal and Photocatalytic Treatment. *Journal of Physics: Conference Series*, IOP Publishing, **1664**(1), 012064, 1-15 (2020), doi:10.1088/1742-6596/1664/1/012064.

[42] Jasim, K. M., and Ahmed, L. M., TiO_2 nanoparticles sensitized by safranine O dye using UV-A light system, In *IOP Conference Series: Materials Science and Engineering*, IOP Publishing, **571**(1), 012064, 1-9 (2019), doi:10.1088/1757-899X/571/1/012064 .

[43] Jawad, T. M., and Ahmed, L. M., Synthesis of WO_3/TiO_2 nanocomposites for Use as Photocatalysts for Eosin Yellow Dye Degradation, acceptance in IOP Conference Series: Materials Science and Engineering, **106**, 012153, 1-12, (2021) . doi:10.1088/1757-899X/1067/1/012153.

[44] Ahmed, L. M., Hussein, F. H., Quantum yield of formaldehyde formation from methanol in the presence of TiO_2 and platinized TiO_2 photocatalysts. Journal of Babylon University/Pure and Applied Sciences/ College of Science/ Babylon University Scientific Conference, **22**(1), 464- 470 (2012).

[45] Oelgemöller, M., and Shvydkiv, O., Recent Advances in Microflow Photochemistry, *Molecules*, **16**, 7522-7550 (2011), https://doi.org/10.3390/molecules16097522.

[46] Chu, W., Jafvert, C., Photodechlorination of Polychlorobenzene Congeners in Surfactant Micelle Solutions, *Environ. Sci. Technol.*, **28**, 2415-2422 (1994), https://doi.org/10.1021/es00062a029.

[47] Chu, W., Jafvert, C., Diehl, C., Marley, K., Larson, R A, phototrans -formations of polychlorobiphenyls in brij 58 micellar solutions, *Environ. Sci. Technol*., **32**,1989-1993 (1998), https://doi.org/10.1021/es970960u.

[48] Ahmed, L. M., Jassim, M. A., Mohammed, M. Q., & Hamza, D. T., Advanced oxidation processes for carmoisine (E122) dye in UVA/ZnO system: Influencing pH, temperature and oxidant agents on dye solution. *Journal of Global Pharma Technology*,**10**(7), 248-254 (2018).

[49] Ahmed, L. M., Saaed, S.I. and Marhoon, A.A., Effect of Oxidation Agents on Photo-Decolorization of Vitamin B 12 in the Presence of ZnO/UV-A system. *Indonesian Journal of Chemistry*, **18**(2), 272-278 (2018), DOI: 10.22146/ijc.33470.

[50] Ahmed, L. M., Alkaim, A. F., Halbus A. F., and Hussein, F. H., Photocatalytic hydrogen production from aqueous methanol solution over metallized TiO_2, *Int. J. of Chem Tech Resch.* **9**(10), 90-98 (2016).

[51] Saeed, S. I., Taresh, B. H., Ahmed, L. M., Haboob, Z. F., Hassan, S. A., and Al-Amir, A. A., Insight into the Oxidant Agents Effect of Removal and Photo-decolorization of Vitamin B_{12} Solution in Drug Tablets using ZrO_2 / acceptance in Journal of Chemical Health Risks, (2021).

[52] Eesa, M. T., Juda, A. M., and Ahmed, L. M., Kinetic and Thermodynamic Study of the Photocatalytic Decolourization of Light Green SF Yellowish (Acid Green 5) Dye using Commercial Bulk Titania and Commercial Nanotitania, *International Journal of Science and Research IJSR*, **5**(11), 1495-1500 (2016), DOI: 10.21275/ART20163016 .

[53] Ahmed, L. M., Tawfeeq, F. T., Abed Al-Ameer, M. H., Abed Al-Hussein, K., and Athaab, A. R., Photo-Degradation of Reactive Yellow 14 Dye (A Textile Dye) Employing ZnO as Photocatalyst, *J. of Geoscience and Environment Protection*, , **4**, 34-44 (2016), DOI: 10.4236/gep.2016.411004 .

[54] Fathal, E. S., and Ahmed, L. M., Optimization of Photocatalytic Decolourization of Methyl Green Dye Using Commercial Zinc Oxide as catalyst, *Journal of Kerbala University, Scientific*, **13**(1), 53-63 (2015).

[55] Hussein, Z. A., Abbas, S. K., and Ahmed, L. M., UV-A activated ZrO_2 via photodecolorization of methyl green dye, In *IOP Conference Series: Materials Science and Engineering*, **454**(1), 012132, IOP Publishing, 1-11(2018), doi:10.1088/1757-899X/454/1/012132.

[56] Jawad, T. M., AL-Lami, M. R., Hasan, A. S., Al-Hilfi, J. A., Mohammad R. K., and Ahmed, L. M., Synergistic effect of dark and photoreactions on the removal and photo-decolorization of azo carmoisine dye (E122) as food dye using Rutile-TiO_2 suspension, Submitted in *Egypt. J. Chem*., (2021), DOI: 10.21608/ejchem.2021.67501.3459.

[57]Alkahlawy, A. A., El-Salamony, R. A., Gobara H. M., Photocatalytic Degradation of Congo Red Dye via Multi-Walled Carbon Nanotubes Modified CuO and ZnO Nanoparticles under Visible Light Irradiation, *Egypt. J. Chem*., **64**(3), pp. 1481 - 1494 (2021), DOI: 10.21608/ejchem.2020.47684.2985 .

[58] Putri, R. A., Safe, S., Jamarun, N., and Septiani, U., Kinetics Study and Degradation Pathway of Methyl Orange Photodegradation in The Presence of C-N-codoped TiO_2 Catalyst, *Egypt.J.Chem*., 62, Special Issue (Part 2), 563 - 575 (2019).

[59] Hanna, A.A., Mohamed, W.A.A. and Ibrahim, I.A., Studies on Photodegradation of Methylene Blue (MB) by Nano-sized Titanium Oxide, *Egypt.J.Chem*., **57**(4), 315-325(2014), DOI: 10.21608/ejchem.2014.1055 .

[60] Hassaan, M. A., Elkatory, M. R. , Ali, R. M., El Nemr, A., Photocatalytic Degradation of Reactive Black 5 Using Photo-Fenton and ZnO Nanoparticles under UV Irradiation, *Egypt.J.Chem.*, **63**(4), 1443-1459 (2020), DOI: 10.21608/ejchem.2019.15799.1955 .